Original Article

METAL (II) COMPLEXES OF ONO DONOR SCHIFF BASE LIGAND AS A NEW CLASS OF BIOACTIVE COMPOUNDS CONTAINING INDOLE CORE: SYNTHESIS AND CHARACTERIZATION

NAGESH GUNVANTHRAO YERNALE, BENNIKALLU HIRE MATHADA MRUTHYUNJAYASWAMY*

*Department of Studies and Research in Chemistry, Gulbarga University, Kalaburagi 585106, Karnataka, India
Email: bhmmswamy53@rediffmail.com

ABSTRACT

Objective: The present communication deals with the synthesis and characterization of biologically active Cu (II), Co (II), Ni (II) and Zn (II) complexes of ONO donor Schiff base ligand derived from the condensation of 5-methyl-3-phenyl-1*H*-indole-2-carbohydrazide with 2-hydroxy-1-napthaldehyde.

Methods: The chemical structures of the Schiff base ligand and its metal complexes were elucidated by elemental analysis and various physicochemical techniques like IR, ^{1}H NMR, ESI mass, double beam UV-visible spectra, ESR, thermal analysis, powder XRD, conductometric and magnetic susceptibility measurements. Newly synthesized compounds were screened for their antibacterial and antifungal activities.

Results: Spectral investigations suggested octahedral coordination geometrical arrangement for Cu (II), Co (II) and Ni (II) complexes, having 1:2 stoichiometric ratio of the type [M(L)$_2$] whereas the tetrahedral coordination geometric arrangement of Zn(II) complex, with 1:1 stoichiometric ratio of the type [Zn(L)Cl]. The antimicrobial activity results revealed that the metal complexes were found to be more active than the free ligand. Furthermore, the DNA cleavage activity was also studied using plasmid DNA pBR322 as a target molecule, and the compounds showed moderate activity.

Conclusion: A new Cu (II), Co (II), Ni (II) and Zn (II) complexes were prepared with tridentate ONO donor novel Schiff base ligand **(L)** and characterized by various physicochemical techniques and all the complexes are found to be non-electrolytic in nature. In addition, all the newly prepared compounds are found to be biologically active.

Keywords: Indole, 2-hydroxy-1-napthaldehyde, Transition metal complexes, Antimicrobial, DNA cleavage, Powder XRD, ESR, Thermal analysis.

INTRODUCTION

A significant growing attention in the synthesis of new metal complexes as drugs and symptomatic agents is presently observed in the field of medicinal inorganic chemistry [1]. A lot of research work in this field is mainly focused on the speciation of metal ions in the biological media based on the possible interaction of different metal ions with different biomolecules, which may lead to the development of new therapeutics or diagnostic agents [2,3]. Several reports revealed that a wide variety of metallic elements play a vital role in biological systems [4-6]. The characteristic property of metals is that they readily lose electrons from the familiar elemental/metallic states to form positively charge ions, which tend to be readily soluble in biological fluids and the metal in this cationic form play a role in the biological system. Metal ions are electron deficient, but most of the biomolecules such as DNA and proteins are electron rich. The general tendency of the attraction of these oppositely charged species will make these ions bind and interact with various biomolecules [7].

Indole and its derivatives are drawing the interest of the researchers for the development of newer drugs owing to their wide variety of biological activities such as antimicrobial [8], anti-malarial [9], anticonvulsant [10], anti-inflammatory [11], anti vascular [12], chronic diabetes [13], HIV inhibitors [14]and particularly in the treatment of cancer [15]. Furthermore, numerous reports suggest that indole 2-carbohydrazides and associated compounds may exhibit antihistaminic [16], antidepressant [17] and antimicrobial activities [18]. On the other hand, Schiff bases derived from 2-hydroxy-1-napthaldehyde have been studied extensively due to their wide range of biological applications [19, 20]. Furthermore, Schiff bases containing 2-hydroxy-1-napthaldehyde group forms stable complexes with various metal ions due to the presence of a phenolic hydroxyl group at their *o*-position, which coordinates to the metal ion *via* deprotonation. Recently, we have reported the synthesis, spectral characterization, thermal study and biological screening of some metal (II) complexes derived from the Schiff base containing

thiazole moiety [21-23]. Furthermore, a survey of the literature reveals that no work has been carried out on the synthesis of metal complexes with Schiff base ligand derived from 5-methyl-3-phenyl-1*H*-indole-2-carbohydrazide and 2-hydroxy-1-napthaldehyde. In the present manuscript we hereby report the synthesis, characterization, thermal and biological relevance of novel Schiff base ligand N'-((2-hydroxynaphthalen-1-yl) methylene)-5-methyl-3-phenyl-1*H*-indole-2-carbohydrazide **(L)**, containing azomethine nitrogen, amide carbonyl and the oxygen atom of the naphthol group as potential cheating sites and its Cu (II), Co (II), Ni (II) and Zn (II) complexes and to investigate their antimicrobial and DNA cleavage properties.

MATERIALS AND METHODS

Materials

All chemicals and solvents were of commercial reagent grade and used as received from Sigma-Aldrich. The metal and chloride contents of the complexes were determined as per standard methods [24]. Precursor molecule 5-methyl-3-phenyl-1*H*-indole-2-carbohydrazide was prepared by the literature method [25].

Elemental analyses were performed by using a Vario EL III CHNS analyzer. FT-IR spectra (4000 to 250 cm^{-1}, KBr pellets) were recorded on a Perkin-Elmer Spectrum RX-I FTIR spectrophotometer. ^{1}H NMR spectra was recorded on Bruker AVANCE II, 400 MHz spectrometer using d_6-DMSO as solvent. Proton chemical shifts are reported in ppm relative to an internal standard of Me$_4$Si. ESI mass spectra were recorded on a mass spectrometer equipped with electro spray ionization (ESI) source having the mass range of 4000 amu in quadruple and 20,000 amu in Tof. Electronic spectra were obtained on an ELICO SL-164 double beam UV-visible spectrophotometer (ca. 10^{-3} M in DMF). Molar conductivity of freshly prepared ca. 10^{-3} M DMF solution of metal complexes was measured using an Elico-CM180 Conductivity Bridge. Electron spin resonance (ESR) measurements of solid [Cu(L)$_2$] complex were carried out on a

BRUKER Bio Spin spectrometer working at a microwave frequency of 8.75-9.65 GHz is using 2,2-diphenylpyridylhydrazone (DPPH) as reference with field set at 3000 Gauss using tetracynoethylene as the 'g' marker (g = 2.00277). TGA/DTA plots were obtained using Perkin Elmer thermal analyzer in flowing N_2 with a heating rate of 20 °C min^{-1}. The magnetic susceptibility measurements were determined on a Gouy balance at room temperature using Hg [Co $(SCN)_4$] as the calibrant. Powder XRD patterns were recorded on Bruker AXS D8 Advance diffractometer.

Synthesis of *N'*-((2-hydroxynaphthalen-1-yl) methylene)-5-methyl-3-phenyl-1*H*-indole-2-carbohydrazide (L)

The Schiff base ligand (L) has been synthesized by refluxing an equimolar mixture of a hot ethanolic solution of 5-methyl-3-phenyl-1*H*-indole-2-carbohydrazide (0.001 mol) and 2-hydroxy-1-napthadlehyde (0.001 mol) (30 ml) with an addition of a catalytic amount of glacial acetic acid (2-3 drops) for about 5-6 h. The characteristic pale yellow colored product, which separated in hot was filtered, washed with hot ethanol, dried and crystallized from hot 1, 4-dioxane. The pathway for the synthesis of Schiff base ligand (L) is presented in Scheme 1.
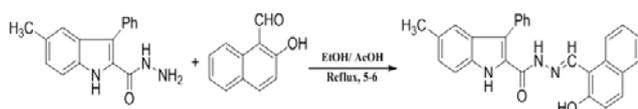
Scheme 1: Synthesis of N'-((2-hydroxynaphthalen-1-yl) methylene)-5-methyl-3-phenyl-1*H*-indole-2-carbohydrazide (L)

Synthesis of metal Schiff base complexes

The hot pale yellowish solution of **L** in 20 ml of ethanol (0.001 mol) was taken in RB flask; a solution of the respective metal (II) chlorides (0.001 mol) in 20 ml of ethanol was added. The reaction mixture was heated under reflux for about 6-7 h. The pH of the reaction mixture adjusted (ca.7.0-7.5) by adding sodium acetate (0.5 g) and reflux is continued for about an hour more. The reaction mixture was cooled to room temperature and poured into distilled water. The resultant precipitate was filtered, washed several times with distilled water, then with hot ethanol to remove any traces of un-reacted starting materials and dried in a vacuum over fused calcium chloride in the desiccator.

Biological activity

Antibacterial and antifungal assay

The antimicrobial activity of **L** and its Cu (II), Co (II), Ni (II) and Zn (II) complexes have been studied for their antibacterial and antifungal activities by using Muller-Hinton agar and potato dextrose agar (PDA) diffusion methods respectively. These activities were carried out in four different concentrations (100, 50, 25 and 12.5 μg/ml in DMSO solvent). The antibacterial activity was tested against four bacteria [*Staphylococcus aureus* (MTCC 3160), *Bacillus subtilis* (MTCC 736), *Escherichia coli* (MTCC 46) and *Salmonella typhi* (MTCC 98)] and antifungal activity against four fungi [*Candida albicans* (MTCC 227), *Cladosporium oxysporum* (MTCC 1777), *Aspergillus flavus* (MTCC 1883) and *Aspergillus Niger* (MTCC 1881)] by a minimum inhibitory concentration (MIC) method [26]. The lowest concentration of each tested compound where the growth of bacteria/fungi was clearly inhibited is reported as MIC. The obtained results were compared under similar conditions using Gentamycin and Fluconazole, a broad-spectrum antibiotic for bacterial and fungal strains respectively. The experiment was done in triplicate, and the average values were calculated.

DNA cleavage studies

The DNA cleavage experiment was conducted using supercoiled plasmid DNA pBR322 as a target molecule as per the literature method [27].

Agarose gel electrophoresis (AGE) method

Each test compound (100 μg) was added separately to the 225 μg of DNA sample, and these sample mixtures were incubated at 37 °C for 2 h. The 600 mg of agarose was dissolved in 60 ml of TAE buffer (4.84 g Tris base, pH 8.0, 0.5 M EDTA L^{-1}) and heated to boil for a few minutes. When the gel attains approximately 55 °C, it was then poured into glass cassette fitted with a comb. The gel was allowed to solidify by cooling to room temperature and then carefully comb was removed. The solidified gel was placed in the electrophoresis chamber flooded with TAE buffer. The 20 μL of DNA sample (mixed with bromophenol blue dye at 1:1 ratio) was loaded into the electrophoresis chamber wells along with standard DNA marker and constant 50 V of electricity was supplied for around 30 min. The gel was removed carefully, stained with ethidium bromide (EtBr) solution (10 μg/ml) for 10-15 min and bands were observed under UV-transilluminator (UVP, Germany) and photographed to determine the extent of DNA cleavage and the results were compared with the standard DNA marker.

RESULTS AND DISCUSSION

Chemistry

The synthesized Cu (II), Co (II), Ni (II) and Zn (II) complexes are colored solids, stable at room temperature and infusible at high temperatures. The complexes are insoluble in water and many common organic solvents, but soluble to a large extent in DMF and DMSO. The elemental analysis data depicted in table 1, are agreeing well with the proposed composition of **L** and its metal complexes. These data support the metal to ligand stoichiometric ratio of the complexes is 1:2 of the type [M $(L)_2$] (M = Cu, Co and Ni) and 1:1 stoichiometry of the type [Zn(L)Cl] for Zn complex (where, '**L**' stands for a deprotonated ligand). The observed molar conductance values are too low to account for any dissociation of the metal complexes indicating that complexes are non-electrolytic in nature.

Table 1: Physical and analytical data of Schiff base ligand (L) and its metal complexes

Compounds	M. W.	M. P. (°C)	Elemental Analysis, found (Calc.) [%]					λ_m	μ_{eff} (BM)
			C	H	N	M	Cl		
$C_{27}H_{21}N_3O_2$ **(L)**	419	280	77.36 (77.32)	5.11 (5.01)	10.14 (10.02)	--	--	--	--
[Cu$(C_{27}H_{20}N_3O_2)_2$] [Cu$(L)_2$]	899.54	>300	72.09 (72.03)	4.32 (4.44)	9.44 (9.33)	7.14 (7.06)	--	21	1.83
[Co$(C_{27}H_{20}N_3O_2)_2$] [Co$(L)_2$]	894.93	>300	72.51 (72.40)	4.35 (4.46)	9.44 (9.38)	6.65 (6.58)	--	19	4.83
[Ni$C_{27}H_{20}N_3O_2)_2$] [Ni$(L)_2$]	894.69	>300	72.54 (72.42)	4.40 (4.47)	9.49 (9.38)	6.69 (6.56)	--	20	2.97
[Zn$(C_{27}H_{20}N_3O_2)$Cl] [Zn(L)Cl]	518.40	>300	62.51 (62.49)	3.75 (3.85)	8.15 (8.10)	12.71 (12.61)	6.62 (6.75)	22	Dia.

IR spectral studies

The IR spectrum of **L**, displayed a broadband at 3431 cm^{-1}, high-intensity strong bands at 1684 cm^{-1}, 1633 cm^{-1} and 1215 cm^{-1} are due to phenolic OH, amide carbonyl function ν (C=O), azo methine function ν (C=N) and phenolic C-O respectively. The medium intensity weak bands observed at 3281 cm^{-1} and 3109 cm^{-1} are due to amide NH and indole NH respectively.

In comparison with the IR spectra of the **L** with that of metal complexes, it was observed that the absence of an absorption band due to phenolic OH at 3431 cm^{-1} of ligand in all the complexes indicates the formation of a coordination bond between the metal ion and phenolic oxygen atom *via* deprotonation. This is further confirmed by an increase in the absorption frequency about 23-75 cm^{-1} of phenolic ν (C-O) which appeared in the region 1238-1290 cm^{-1} in all the metal complexes indicating the participation of an oxygen atom of the phenolic OH in the coordination and formation of the metal-oxygen bond. The most notable change is the shift of amide carbonyl ν(C=O) to lower frequency side about 85-29 cm^{-1} which appeared in the region 1599-1655 cm^{-1} in all the complexes confirm coordination of an oxygen atom of the amide ν(C=O) with the metal ions as such without undergoing enolization [28] Also, the shift of

azomethine ν(C=N) function to lower frequency side about 76-13 cm^{-1} and appeared in the region 1557-1620 cm^{-1} in all the metal complexes indicating the involvement of nitrogen atom of azomethine function in coordination [29].

The medium intensity weak bands observed at 3276-3291 cm^{-1} and 3100-3114 cm^{-1} were due to amide NH and indole NH respectively, which appeared almost at about the same region as in the case of **L**, confirms their non-involvement in coordination.

Appearance of new weak intensity, non-ligand bands in the region 519-545 cm^{-1}, 471-493 cm^{-1} in all the complexes and at 329 cm^{-1} (in case of [Zn(L)Cl]) in the IR spectra of metal complexes are assigned to frequencies of ν(M-O), ν(M-N) and ν(M-Cl) stretching vibration respectively. The prominent IR spectral data are listed in table 2.

Table 2: IR spectral data (cm^{-1}) of Schiff base ligand (L) and its metal complexes

Ligand/ Complexes	ν OH (Phenolic)	ν NH (Indole)	ν NH (Amide)	ν C=O	ν C=N	ν C-O	ν M-O	ν M-N	ν M-Cl
L	3431	3281	3109	1684	1633	1215	--	--	--
[Cu(L)₂]	--	3288	3100	1614	1581	1249	522	492	--
[Co(L)₂]	--	3286	3100	1655	1620	1238	519	493	--
[Ni(L)₂]	--	3276	3114	1599	1557	1290	534	471	--
[Zn(L)Cl]	--	3291	3112	1654	1582	1242	545	478	329

¹H NMR spectral studies

The ¹H NMR spectrum of **L** displayed three singlets each at 12.6, 11.8 and 11.7 ppm are ascribed to protons of phenolic OH, amide NH and indole NH respectively. A characteristic singlet appeared at 9.2 ppm is assigned to azo methine proton (HC=N). In addition to this, the fourteen aromatic protons have resonated as a multiplet in the region 7.1-8.2 ppm and signal at 2.4 ppm is due to three protons of the methyl group of the indole moiety. The ¹H NMR spectrum of [Zn (L) Cl] displayed two singlets each at 12.2 and 11.6 ppm are ascribed to protons of amide NH and indole NH respectively. A characteristic singlet proton signal at 10.6 ppm is assigned to azo methine proton (HC=N). In addition to this, the fourteen aromatic protons have resonated as a multiplet in the region 7.2-8.3 ppm and signal at 2.6 ppm is due to three protons of the methyl group of the indole moiety.

In comparison, the most notable change is observed in the ¹H NMR spectrum [Zn (L) Cl] complex is the disappearance of signal due to the proton of phenolic OH substantiates the involvement and bonding of a phenolic oxygen atom to metal ion *via* deproteination. Also, the signals due to all the protons have been shifted towards down field strength proves the coordination of Zn (II) ion with **L**.

ESI mass spectral studies

The ESI mass spectrum of the **L** showed M$^+$+1 peak at 420 (100%), which is also a base peak. Similarly, the ESI mass spectra of [Cu (L)₂] and [Ni(L)₂] complexes displayed a molecular ion peak recorded at M$^+$ 899 (2%) and M$^+$ 894 (2%) respectively, which are equivalent to their molecular weights.

Mass spectral fragmentation pattern study of Schiff base ligand (L)

The ESI mass spectrum of **L** displayed M$^+$+1 peak at 420 (100%), which is also a base peak. The M$^+$ molecular ion peak recorded at m/z 419 (1%) undergone a fragmentation by two routes, first on loss of C$_{10}$H$_7$O radical and the H$_2$ molecule gave a fragment ion peak recorded at m/z 274 (3%). Further, this on the loss of CHN$_2$ and CH$_3$ radicals simultaneously gave a fragment ion peak recorded at m/z 218 (4%). Another route, the molecular ion underwent fragmentation and gave a peak recorded at m/z 338 (4%) which is due to the loss of the benzene molecule of the indole moiety, a hydrogen radical and two H atom. This schematic mass spectral fragmentation pattern of **L** is in consistency with its structure, Scheme 2.
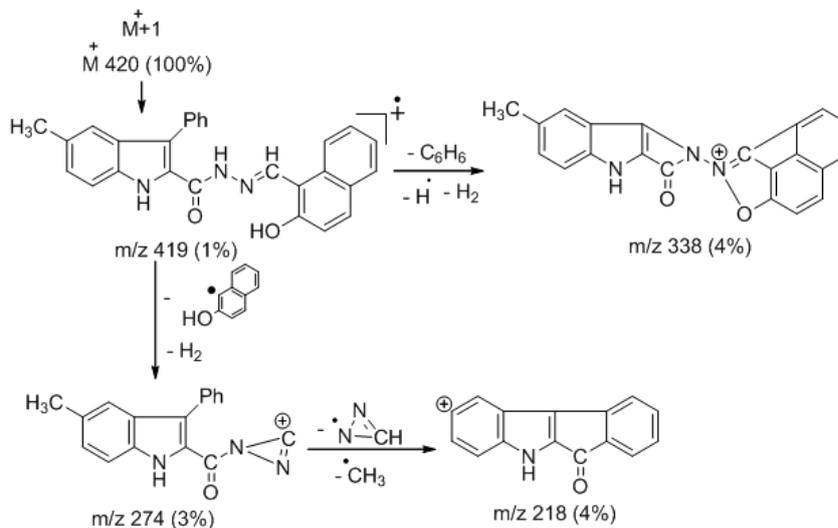
Scheme 2: Mass spectral fragmentation pattern of L

Electronic spectral studies

The information regarding the proposed geometry of the metal complexes was confirmed from their electronic absorption spectral study and magnetic susceptibility measurement data, table 3. The electronic spectra of green colored [Cu (L)$_2$] complex displayed a low-intensity single broad asymmetric band in the region 15426-17867 cm^{-1}. The broadness of the band designates the three transitions $^2B_{1g} \rightarrow {}^2A_{1g}$ (ν_1), $^2B_{1g} \rightarrow {}^2B_{2g}$ (ν_2) and $^2B_{1g} \rightarrow {}^2E_g$ (ν_3), which are similar in energy and give rise to only one broadband and the broadness of the band may be due to dynamic Jahn-Teller distortion. The obtained data suggest the distorted octahedral geometry around the Cu (II) ion [30].

The brown colored [Co (L)$_2$] complex displayed two absorption bands at 16760 cm^{-1} and 19892 cm^{-1}. These bands are assigned to be $^4T_{1g}$ (F) $\rightarrow {}^4A_{2g}$ (F) (ν_2) and $^4T_{1g}$ (F) $\rightarrow {}^4T_{2g}$ (P) (ν_3) transitions, respectively, which are in good agreement with the literature values for octahedral geometry [31]. The lowest band, ν_1 could not be observed due to the limited range of the instrument used, but it could be calculated using the band fitting procedure suggested by Underhill and Billing [32]. The transition values of ν_1, ν_2 and ν_3 suggest the octahedral geometry for [Co (L)$_2$] complex.

The brown colored [Ni(L)$_2$] complex exhibited two absorption bands in the region 15735 cm^{-1} and 25563 cm^{-1}, which are assigned to $^3A_{2g} \rightarrow {}^3T_{1g}$ (F) (ν_2) and $^3A_{2g}$ (F) $\rightarrow {}^3T_{1g}$ (P) (ν_3) transitions respectively in an octahedral environment [33]. The transition value of band ν_1 was also calculated by using a band fitting procedure [32]. The orange-colored [Zn (L)(Cl)] complex is found to be accordingly diamagnetic in nature, it is proposed to have a tetrahedral geometry.

The proposed octahedral geometry of [Cu(L)$_2$], [Co(L)$_2$] and [Ni(L)$_2$] complexes was further supported by the calculated values of ligand field parameters, such as Racah interelectronic repulsion parameter (B′), nephelauxetic parameter (β), ligand field splitting energy (10 Dq) and ligand field stabilization energy (LFSE) [34]. The calculated B′ values for the [Co (L)$_2$] and [Ni(L)$_2$] complexes are lower than the free ion values, which is due to the orbital overlap and delocalization of d-orbitals. The β values are important in determining the covalency for the metal-ligand bond, and they were found to be less than unity, suggesting a considerable amount of covalency for the metal-ligand bonds. The β value for the [Ni(L)$_2$] complex was less than that of the [Co(L)$_2$] complexes, indicating the greater covalency of the Metal-Ligand (M-L) bond.

Table 3: Electronic spectral data and ligand field parameters of the [Cu(L)$_2$], [Co(L)$_2$] and [Ni(L)$_2$] complexes

| Complexes	Transitions in cm^{-1}			Dq (cm^{-1})	B′ (cm^{-1})	β	β%	ν_2/ν_1	LFSE (k cal.)
	$\nu_1{}^*$	ν_2	ν_3						
[Cu(L)$_2$]	15426-17867			--	--	--	--	--	28.53
[Co(L)$_2$]	7820	16760	19892	894	879	0.905	9.47	2.14	15.32
[Ni(L)$_2$]	9830	15735	25563	983	785	0.754	24.51	1.60	33.70

*Calculated values

Magnetic susceptibility studies

For the complexes [Cu (L)$_2$], [Co(L)$_2$] and [Ni(L)$_2$], the magnetic susceptibility measurements were carried out, and obtained data are presented in table 1 and they were found to be paramagnetic in nature. The obtained magnetic moment value for [Cu (L)$_2$] complex is 1.83 BM. This value is slightly higher than the spin-only value 1.73 BM due to one unpaired electron, suggesting the octahedral geometry for [Cu (L)$_2$] complex [35]. Thus, the present [Cu (L)$_2$] complex is devoid of any spin interaction with distorted octahedral geometry. In octahedral [Co (L)$_2$] complex the ground state is $^4T_{1g}$. A large orbital contribution to the singlet state lowers the magnetic moment values for the various [Co (L)$_2$] complexes, which are in the range 4.12-4.70 for tetrahedral and 4.70-5.20 BM for the octahedral geometry of the complexes respectively [36]. In the present study, the observed magnetic moment value is 4.83 BM suggests the octahedral geometry. Further, the observed magnetic moment value for [Ni (L)$_2$] complex is 2.97 BM, which is also well within the expected range of 2.83-3.50 BM, suggesting the consistency with its octahedral environment [37].

ESR spectral study of [Cu (L)$_2$] complex

The ESR spectrum provides the evidence about the environment of the metal ion within the complex, i.e., the geometry and nature of the ligating sites of the ligand and metal ion. In octahedral geometry with the g-tensor parameter $g_\perp > g_{||} > 2.0023$, the unpaired electron lies in the d_{z^2} orbital and $g_{||} > g_\perp > 2.0023$, the unpaired electron lies in the $d_{x^2-y^2}$ orbital in the ground-state [38]. The observed measurements of [Cu(L)$_2$] complex are $g_{||}$ (2.1394) > $g_\perp$ (2.0316) > 2.0023 indicate that the complex is an axially symmetric and the copper site has a $d_{x^2-y^2}$ ground state characteristic of octahedral geometry [39]. The $g_{||}$ value is an important function for indicating the metal-ligand (M-L) bond character, for covalent and ionic character $g_{||}$ value < 2.3 and $g_{||}$ value > 2.3 respectively [40]. In the present case, $g_{||}$ value of [Cu (L)$_2$] complex is < 2.3, indicating an appreciable covalent character for the M-L bond.

The geometric parameter (G) is the measure of the extent of exchange interactions and is calculated by using the g-tensor values by using the expression G = $g_{||}$-2.0023/$g_\perp$-2.0023. According to

Hathaway and Billing [41], if the G value is greater than 4, the exchange interaction between the copper centers is negligible, whereas if its value is less than 4 and the exchange interaction is noticed. In present investigations, it was found that G value is 4.68, indicate the exchange coupling effects are not operative. The ESR spectra of [Co(L)$_2$], [Ni(L)$_2$] and [Zn(L)(Cl)] complexes at room temperature, do not show ESR signals because the rapid spin-lattice relaxation of the [Co(L)$_2$] and [Ni(L)$_2$] complexes, which broadens the lines at a higher temperature [42] and the diamagnetic nature of the [Zn(L)(Cl)] complex. Generally, the ESR spectra show signals that may be accounted for the presence of free radicals that can result from the cleavage of any double bond and distribution of the charge on the two neighbor atoms. The presence of unpaired electrons from any source inside the molecule can be responsible for the appearance of this signal [43].
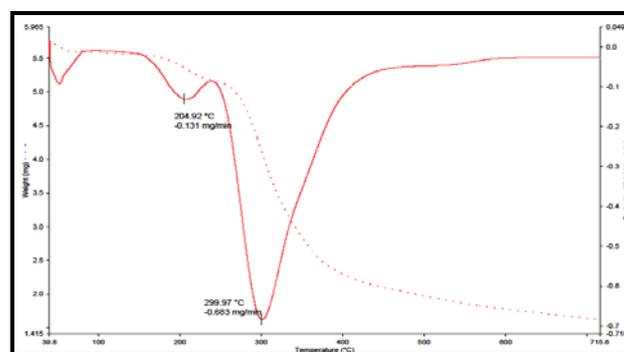
Fig. 1: TGA-DTA curve of [Cu (L)$_2$] complex

Thermal studies

The thermogram of [Cu(L)$_2$] complex (fig. 1), specifies that the complex is steady up to 274 °C, no weight loss occurred before this temperature. The complex underwent degradation in three succeeding stages. The first stage of degradation occurred at 275 °C, due to the

loss of two phenyl groups of indole moieties (Obs. 15.00%, Calc. 17.11%). The resultant complex on further degradation furnished a break at 325 °C by the loss of two $C_{10}H_6$ species (Obs. 33.45%, Calc. 33.80%). Further, the resulting complex underwent the third stage of decomposition at 386 °C due to loss of $C_{10}H_7NO$ molecule of indole moiety (Obs. 30.72%, Calc. 31.81%). Further, complex showed steady decomposition up to 715 °C and onwards due to the loss of remaining

organic moiety. The final weight of the residue corresponds to cupric oxide. Similarly, $[Co(L)_2]$, $[Ni(L)_2]$ and $[Zn(L)Cl]$ complexes underwent a decomposition in various stages due to the loss of different organic moieties with respect to temperature, table 4. The results are in good agreement with the formulae suggested from the physical and analytical data.

**Table 4: Thermal degradation pattern of metal (II) complexes**

Metal Complexes	Temp. (°C)	Weight loss (%)		Metal oxide (%)		Inference
		Obs.	Calc.	Obs.	Calc.	
$[Cu(L)_2]$	275	15.00	17.11	--	--	Loss due to two phenyl groups of indole moieties.
	325	33.45	33.80	--	--	Loss due to two $C_{10}H_6$ species.
	386	30.72	31.81	--	--	Loss due to $C_{10}H_7NO$ molecule of indole moiety.
	Up to 715	--	--	11.95	12.45	Loss due to remaining organic moiety
$[Co(L)_2]$	304	8.62	8.60	--	--	Loss due to a phenyl group.
	406	13.02	13.08	--	--	Loss due to a phenyl group and two CH_3 species of indole moieties.
	427	39.13	39.10	--	--	Loss due to two $C_{11}H_7$ species.
	477	26.78	26.56	--	--	Loss due to C_8H_5N species.
	Up to 715	--	--	12.34	13.97	Loss due to remaining organic moieties.
$[Ni(L)_2]$	311	4.43	3.35	--	--	Loss due to two CH_3 groups of indole carboxamide moieties.
	343	52.92	54.35	--	--	Loss due to two moles of $C_{15}H_{11}N_2O$ molecule of indole moieties.
	411	31.55	31.92	--	--	Loss due to $C_{10}H_6$ species.
	Up to 716	--	--	10.67	12.23	Loss due to remaining organic moiety.
$[Zn(L)Cl]$	257	5.50	6.75	--	--	Loss due to a coordinated chlorine atom.
	339	51.05	51.71	--	--	Loss due to $C_{16}H_{14}N_2O$ molecule of indole carboxamide moiety.
	432	58.68	59.12	--	--	Loss due to $C_{11}H_6$ species.
	Up to 715	--	--	13.47	14.29	Loss due to remaining organic moiety.

Powder X-ray diffraction studies (Powder-XRD)

Though our newly synthesized metal complexes were soluble only in some polar organic solvents like DMSO and DMF, crystals that are appropriate for single crystal studies are not achieved. In order to test the degree of crystallinity of metal complexes, we obtained the powder X-ray diffraction pattern. In powder X-ray diffraction pattern, it was observed that the trend of curves decreases from maximum to minimum intensity indicating the amorphous nature of the complexes. Powder X-ray diffraction pattern of $[Cu(L)_2]$, $[Co(L)_2]$ and $[Zn(L)Cl]$ complexes displayed an eleven, nine and five reflections respectively, with maxima at 2θ = 36.674, 41.006 and 26.496 corresponding to observed values 2.450 Å, 2.201 Å and 3.364 Å respectively.

The Bragg's equation ($n\lambda=2d \sin\theta$) were used for calculating the interplanar spacing (d). The calculated inter-planar d-spacing together with relative intensities with respect to the most intense peak have been recorded.

From all the high intense peaks, unit cell calculations have been calculated, and $h^2+k^2+l^2$ values were determined. The observed inter-planar d-spacing values have been compared with the calculated one, and it was found to be in good agreement with experimental values. The $h^2+k^2+l^2$ values of $[Cu(L)_2]$ complex are 1, 1, 4, 5, 6, 11, 15, 19, 20, 24 and 36 (fig. 2) and calculated lattice parameter for $[Cu(L)_2]$ complex is a=b=c=14. 818 Å (table 5). The presence of forbidden number15 indicates that the complex may belong to hexagonal or tetragonal systems.
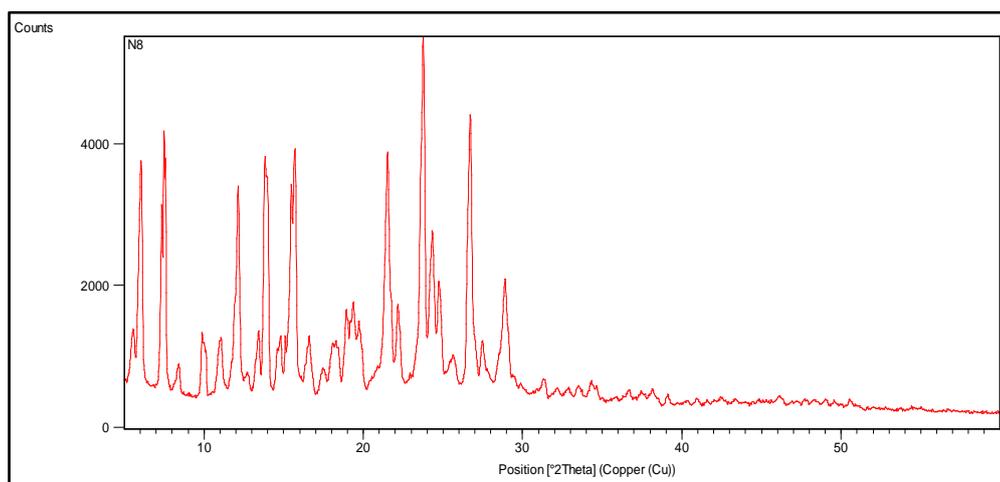
Fig. 2: Powder XRD spectrum of [Cu (L)₂] complex

Similar calculations were done for $[Co(L)_2]$ and $[Zn(L)Cl]$ complexes and all the important peaks have been indexed, and observed values of interplanar distances (d) have been compared with the calculated once, and it was found to be in good agreement. The presence of forbidden number 27 in the case of $[Co(L)_2]$ complex indicated that this complex may belong to hexagonal or tetragonal systems. The absence of forbidden numbers (7, 15, 23, etc.) in $[Zn(L)Cl]$ complex indicates that complex belongs to cubic symmetry. The calculated lattice parameter for $[Co (L)_2]$ and $[Zn(L)Cl]$ complexes are a=b=c=11. 478 Å and a=b=c=14. 058 Å respectively.

Table 5: Powder X-ray data of [Cu (L)₂] complex

Peak	2θ	θ	Sinθ	Sin²θ	1000 Sin²θ	1000 Sin²θ/CF (h²+k²+l²)	h k l	d Obs.	Calc.	a in Å
1	6.048	3.024	0.052	0.002	2.783	1.00 (1)	1 0 0	14.611	14.807	14.818
2	7.355	3.677	0.064	0.004	4.113	1.47 (1)	1 0 0	12.018	12.031	14.579
3	12.717	6.358	0.110	0.012	12.265	4.40 (4)	2 0 0	6.961	7.000	14.623
4	13.825	6.912	0.120	0.014	14.484	5.20 (5)	2 1 0	6.405	6.416	14.637
5	14.805	7.402	0.128	0.016	16.599	5.96 (6)	2 1 1	5.983	6.015	14.634
6	19.951	9.975	0.173	0.030	30.007	10.78 (11)	3 1 1	4.450	4.450	14.596
7	23.582	11.791	0.204	0.041	41.755	15.00 (15)	---	3.772	3.774	14.603
8	26.526	13.263	0.229	0.052	52.634	18.91 (19)	3 3 1	3.360	3.362	14.683
9	27.477	13.738	0.237	0.056	56.401	20.26 (20)	4 2 0	3.246	3.248	14.648
10	29.873	14.936	0.257	0.066	66.434	23.87 (24)	4 2 2	2.990	2.996	14.643
11	36.674	18.337	0.314	0.098	98.976	35.56 (36)	4 4 2	2.450	2.452	14.667

Biological activity results

Antibacterial and antifungal assay results

The newly synthesized compounds have been evaluated for their antibacterial and antifungal activity. The size of inhibition zone (mm) formed at different concentrations of the tested compounds against the respective bacterial and fungal strains along with the standards are summarized in table 6. In most of the cases, it was observed that the metal complexes revealed moderate antimicrobial activity than the free ligand, the activity was found to be improved on the coordination of the hetero atoms (ONO) of the **L** with different metal ions. This enhancement in the antimicrobial activity of the complexes over the free ligand can be explained based on chelation theory [44, 45]. It is known that chelation enhances the ligand to act as more powerful and potent bactericidal/fungicidal agents by inhibiting

the growth of bacteria/fungi, a thus zone of inhibition of metal complexes was found to be higher compared to the ligand. The enhancement in the antimicrobial activity may be rationalized on the basis that ligands mainly possess azomethine group (C=N).

Moreover, in metal complexes, the positive charge of the metal ion is partially shared by the hetero donor atoms (N and O) present in the ligand and there may be π-electron delocalization over the whole chelating system [46, 47].

Hence, the increase in the lipophilic character of the metal chelates favour their permeation through the lipid layer of the bacterial cell membranes and blocking of the metal binding sites for the enzymes of microorganisms. In general, metal complexes are more active than the ligands because metal complexes may serve as a vehicle for activation of ligands as the principal cytotoxic species [48].

Table 6: Size of inhibition zone (mm) formed at different concentrations (12.5, 25, 50 and 100 µg/ml in DMSO solvent) against various Bacteria and fungi

Compounds	Bacteria				Fungi			
	B. Subtilis	*S. aureus*	*E. coli*	*S. typhi*	*C. albicans*	*C. oxysporum*	*A. Flavus*	*A. niger*
L	10.09±0.12	11.10±0.11	10.34±0.52	9.59±0.32	9.19±0.34	10.10±0.21	12.21±0.09	10.09±0.22
[Cu(L)₂]	13.12±0.53	13.49±0.23	12.20±0.10	10.41±0.12	10.10±0.32	12.12±0.32	14.34±0.13	13.11±0.31
[Co(L)₂]	12.26±0.24	12.36±0.24	13.21±0.24	12.26±0.23	12.31±0.31	11.16±0.40	14.12±0.18	13.12±0.12
[Ni(L)₂]	13.34±0.58	12.34±0.58	12.34±0.28	11.24±0.36	11.23±0.10	12.14±0.15	13.21±0.24	14.23±0.16
[Zn(L)Cl]	12.69±0.43	11.69±0.03	12.19±0.51	12.19±0.33	12.13±0.32	11.09±0.22	14.09±0.11	14.19±0.19
Gentamicin	18.40±0.52	19.53±0.12	18.30±0.52	19.30±0.27	--	--	--	--
Fluconazole	--	--	--	--	19.10±0.12	20.15±0.11	18.34±0.11	19.34±0.31

Note: The stock solutions of the test compounds were prepared by dissolving 10 mg of the test compound in 10 ml of freshly distilled DMSO (1 mg/ml).

DNA cleavage activity

The gel picture (fig. 3) showing the cleavage of plasmid pBR322 DNA molecule. From the figure, it is evident that the **L** and its newly synthesized metal complexes have acted on DNA because of a difference in their molecular weights between the control and the treated DNA sample. The gel electrophoresis clearly revealed that there was a difference in the migration of the lanes of **L**, [Cu(L)₂], [Co(L)₂], [Ni(L)₂] and [Zn(L)Cl] complexes respectively as compared to the control plasmid DNA pBR322 **(C)** at 100 µg/l concentration. It is clearly observed that the lanes of [Cu (L)₂] and [Co(L)₂] complexes showed complete cleavage of supercoiled DNA, whereas **L**, [Ni(L)₂] and [Zn(L)₂] complexes showed partial cleavage of supercoiled DNA. This shows that the control DNA alone does not show any apparent cleavage, whereas the **L** and its metal complexes do show. Based on these outcomes, it can be concluded that all the newly synthesized compounds under present study are good pathogenic microorganism inhibitors.

CONCLUSION

New Cu (II), Co (II), Ni (II) and Zn (II) complexes were prepared with tridentate ONO donor Schiff base ligand **(L)** derived from the condensation of 5-methyl-3-phenyl-1*H*-indole-2-carbohydrazide and 2-hydroxy-1-napthaldehyde and characterized them by various spectral techniques. Spectral study and elemental analysis data

indicate octahedral geometry for Cu (II), Co (II) and Ni (II) complexes having 1:2 stoichiometric ratio of the type [M(L)₂] and tetrahedral geometry for Zn (II) complex having 1:1 stoichiometry ratio of the type [M(L)Cl].

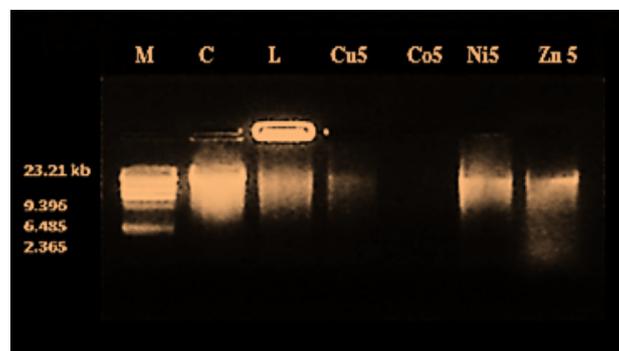
Fig. 3: DNA cleavage on plasmid pBR 322
M: Standard DNA, C: Control DNA (untreated pBR 322), L: Schiff base ligand (L), Cu5: [Cu (L)₂] complex, Co5: [Co(L)₂] complex, Ni5: [Ni(L)₂] complex and Zn5: [Zn(L)Cl] complex

From the biological activity study, it was observed that the antimicrobial activity of all the complexes was found to be enhanced on complexation. Also, DNA cleavage studies revealed that all the compounds showed good efficiency towards DNA cleavage. Hence, from all these extensive observations, it is concluded that the newly prepared **L** and its metal complexes gave remarkable, versatile and valuable information of new coordination compounds and also they may be used as powerful biologically active agents with reduced toxicity and higher efficiency. Based on the physicochemical evidence, we proposed the following structures for the metal complexes.

M = Cu(II), Co(II) and Ni(II)
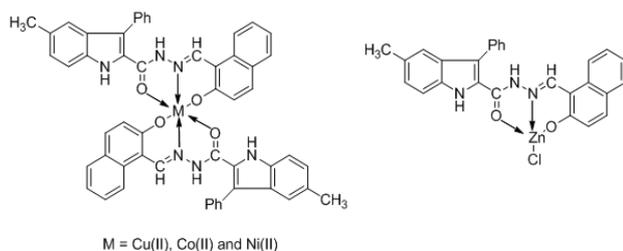
Proposed structures of the metal complexes

ACKNOWLEDGEMENT

CONFLICT OF INTERESTS

Declared none

REFERENCES

1. Thompson KH, Orvig C. Metal complexes in medicinal chemistry: new vistas and challenges in drug design. Dalton Trans 2006;6:761-4.
2. Timerbaev AR, Hartinger CG, Aleksenko SS, Keppler BK. Interactions of antitumor metallodrugs with serum proteins: advances in characterization using modern analytical methodology. Chem Rev 2006;106:2224-48.
3. Ming LJ. Structure and function of "metallo antibiotics". Med Res Rev 2003;23:697-762.
4. Refat MS, El-Sayed MY, Adam AMA. Cu(II), Co(II) and Ni(II) complexes of new schiff base ligand: synthesis, thermal and spectroscopic characterizations. J Mol Struct 2013;1038:62-72.
5. Nejo AA, Kolawole GA, Nejo AO. Synthesis, characterization, antibacterial, and thermal studies of unsymmetrical Schiff-base complexes of cobalt(II). J Coord Chem 2010;63:4398-410.
6. Osredkar J, Sustar N. Copper and Zinc, Biological role and significance of Copper/Zinc Imbalance. J Clin Toxicol 2011;S3:1.
7. Sheikh J, Juneja H, Ingle V, Ali P, Hadda TB. Synthesis and *in vitro* biology of Co (II), Ni (II), Cu (II) and Zinc (II) complexes of functionalized beta-diketone bearing energy buried potential antibacterial and antiviral O, O pharmacophore sites. J Saudi Chem Soc 2011;17:269-76.
8. Al-Quawasmeh RA, Huesca M, Nedunuri V, Peralta R, Wright J, Lee Y, *et al.* Potent antimicrobial activity of 3-(4, 5-diaryl-1H-imidazol-2-yl)-1*H*-indole derivatives against methicillin-resistant Staphylococcus aureus. Bioorg Med Chem Lett 2010;20:3518-20.
9. Mascal M, Modes KV, Durmus A. Concise photochemical synthesis of the antimalarial indole alkaloid decursivine. Angew Chem Int Ed Engl 2011;50:4445-6.
10. Mandour AH, El-Sawy ER, Shaker KH, Mustafa MA. Synthesis, anti-inflammatory, analgesic and anticonvulsant activities of 1,8-dihydro-1-ary1-8-alkyl pyrazolo(3,4-b) indoles. Acta Pharm 2010;60:73-8.
11. Narayana B, Ashalatha BV, Vijayaraj KK, Fernandes J, Sarojini BK. Synthesis of some new biologically active 1,3,4-oxadiazolyl nitro indoles and a modified Fischer indole synthesis of ethyl nitro indole-2-carboxylates. Bioorg Med Chem 2005;13:4638-44.
12. Ty N, Dupeyre G, Chabot GG, Seguin J, Tillequin F, Scherman D, *et al.* Synthesis and biological evaluation of new disubstituted analogs of 6-methoxy-3-(3',4',5'-trimethoxybenzoyl)-1*H*-indole (BPR0L075), as potential antivascular agents. Bioorg Med Chem 2008;16:7494-503.
13. Zandt MCV, Jones ML, Gunn DE, Geraci LS, Jones JH, Sawicki DR, *et al.* Discovery of 3-[(4,5,7-trifluorobenzothiazol-2-yl)methyl]indole-N-acetic acid (lidorestat) and congeners as highly potent and selective inhibitors of aldose reductase for the treatment of chronic diabetic complications. J Med Chem 2005;48:3141-52.
14. Sechi M, Derudas M, Dallocchio R, Dessi A, Bacchi A, Sannia L, *et al.* Design and synthesis of novel indole beta-diketo acid derivatives as HIV-1 integrase inhibitors. J Med Chem 2004;47:5298-310.
15. Chinni SR, Li Y, Upadhyay S, Koppolu PK, Sarkar FH. Indole-3-carbinol (I3C) induced cell growth inhibition, G1 cell cycle arrest and apoptosis in prostate cancer cells. Oncogene 2001;20:2927-36.
16. Merwade AY, Rajur SB, Basanagoudar LD. Synthesis and antiallergic activities of 10-substituted-4-chloro-12-methyl(or phenyl)-1,2-dihydroquinoxalino[1,2-a] indoles. Indian J Chem 1990;29B:1113-7.
17. Fernandez AE, Monge VA. "Spanish Patent 400,436" chemical abstract. Spanish Patent Trademark Office 1975;83:114205.
18. Sinnur KH, Siddappa S, Hiremath SP, Purohit MG. Synthesis of substituted 2-(1 ', 3', 4'-oxadiazol-2'yl) indoles. Indian J Chem 1986;25B:716-29.
19. Jeewoth T, Wah HLK, Bhowon MG, Ghoorohoo D, Babooram K. Synthesis and anti-bacterial/catalytic properties of Schiff bases and Schiff base metal complexes derived from 2,3-diaminopyridine. Synth React Inorg Met-Org Nano-Met Chem 2000;30:1023-38.
20. Yernale NG, Mruthyunjayaswamy BHM. Synthesis, Characterization, Antimicrobial, DNA Cleavage, and *in vitro* cytotoxic studies of some metal complexes of Schiff base ligand derived from thiazole and quinoline moiety. Bioinorg Chem Appl 2014:1-17. doi: 10.1155/2014/314963. [Article in Press]
21. Mahendra Raj K, Vivekanand B, Nagesh GY, Mruthyunjayaswamy BHM. Synthesis, spectroscopic characterization, electrochemistry and biological evaluation of some binuclear transition metal complexes of bicompartmental ONO donor ligands containing benzo[b]thiophene moiety. J Mol Struct 2014;1059:280-93.
22. Nagesh GY, Mahendra Raj K, Mruthyunjayaswamy BHM. Synthesis, characterization, thermal study and biological evaluation of Cu(II), Co(II), Ni(II) and Zn(II) complexes of Schiff base ligand containing thiazole moiety. J Mol Struct 2015;1079:423-32.
23. Nagesh GY, Mahadev UD, Mruthyunjayaswamy BHM. Mononuclear metal (II) schiff base complexes derived from thiazole and *O*-Vanillin moieties: synthesis, Characterization, Thermal behaviour and biological evaluation. Int J Pharm Sci Rev Res 2015;31:190-7.
24. Mendham J, Denney RC, Barnes JD, Thomas MJK. Vogel's Quantitative Chemical Analysis. 6nd ed. Prentice Hall London; 2000.
25. Hiremath SP, Mruthyunjayaswamy BHM, Purohit MG. Synthesis of substituted 2-aminoindolees and 2-(2'-Phenyl-1',3',4'-oxadiazolyl) aminoindoles. Indian J Chem 1978;16B:789-92.
26. Sadana AK, Mirza Y, Aneja KR, Prakash O. Hypervalent iodine mediated synthesis of 1-aryl/hetryl-1,2,4-triazolo[4,3-a] pyridines and 1-aryl/hetryl 5-methyl-1,2,4-triazolo[4,3-a]quinolines as antibacterial agents. Eur J Med Chem 2003;38:533-6.

27. Sambrook J, Fritsch EF, Maniatis T. Molecular cloning: a laboratory manual. 2nd ed. Cold Spring Harbor Laboratory, Cold Spring Harbor (NY); 1989.
28. Roy S, Mandal TN, Das K, Butcher RJ, Rheingold AL, Kar SK. Syntheses, characterization, and X-ray crystal structures of two cis-dioxovanadium (V) complexes of pyrazole-derived, Schiff-base ligands. J Coord Chem 2010;63:2146-57.
29. Chandra S, Gupta LK. Electronic, EPR, Magnetic and mass spectral studies of mono and homo binuclear Co(II) and Cu(II) complexes with a novel macrocyclic ligand. Spectrochim Acta Part A 2005;62:1102-6.
30. Liu H, Wang H, Gao F, Niu D, Lu Z. Self-assembly of copper (II) complexes with substituted aryl hydrazones and monodentate Nheterocycles: synthesis, structure, and properties. J Coord Chem 2007;60:2671-8.
31. Rai RA. Metal complexes of 5-(*o*) hydroxyphenyl-1,3,4-oxadiazole-2-thione. J Inorg Nucl Chem 1980;42:450-3.
32. Underhill AE, Billing DE. Calculations of the racah parameter b for nickel (II) and cobalt (II) compounds. Nature 1966;210:834-5.
33. Bayoumi HA, Alaghaz AMA, Aljahdali MS. Cu(II), Ni(II), Co(II) and Cr(III) Complexes with N2O2-Chelating schiff's base ligand incorporating azo and sulfonamide moieties: spectroscopic, electrochemical behavior and thermal decomposition studies. Int J Electrochem Sci 2013;8:9399-413.
34. Satyanarayana DN. Electronic Absorption Spectroscopy and Related Techniques, University Press: India Limited, (New Delhi); 2001.
35. Singh DP, Kumar R, Malik V, Tyagi P. Synthesis and characterization of complexes of Co(II), Ni(II), Cu(II), Zn(II), and Cd(II) with macrocycle 3,4,11,12-tetraoxo-1,2,5,6,9,10,13,14-octaazacyclo-hexadeca-6,8,14,16-tetraene and their biological screening. Transition Met Chem 2007;32:1051-5.
36. Baranwal BP, Gupta T. Synthesis and physicochemical studies on iron (II,III,III) and cobalt(II) thiocarboxylates. Synth React Inorg Met-Org Chem 2004:34:1737-54.
37. Rao TR, Archana P. Synthesis and spectral studies on 3d metal complexes of mesogenic schiff base ligands. Part 1. Complexes of N-(4-Butylphenyl) salicyl aldimine. Synth React Inorg Met-Org Chem 2005;35:299-304.
38. Balasubramanian S, Krishnan CN. Synthesis and characterization of five-coordinate macrocyclic complexes of nickel (II) and copper (II). Polyhedron 1986;5:669-75.
39. Thaker BT, Tandel PK, Patel AS, Vyas CJ, Jesani MS, Patel DM. Synthesis and mesomorphic characterization of Cu(II), Ni(II) and Pd (II) complex with azomethine and chalcone as a bridging group. Ind J Chem 205;44A:265-70.
40. Kilveson D. Publications of daniel kivelson. J Phys Chem B 1997;101:8631-4.
41. Hathaway BJ, Billing DE. The electronic properties and stereochemistry of mononuclear complexes of the copper (II) ion. Coord Chem Rev 1970;5:143-207.
42. Fouda MFR, Abd-el-zaher MM, Shadofa M, El Saied FA, Ayad MI, El-Tabl AS. Synthesis and characterization of transition metal complexes of N'-[(1,5-dimethyl-3-oxo-2-phenyl-2,3-dihydro-1H-pyrazol-4-yl)methylene]thiophene-2-carbohydrazide. Trans Met Chem 2008;219:219-28.
43. Abdallah SM, Zayed MA, Mohamad GG. Synthesis and spectroscopic characterization of new tetradentate schiff base and its coordination compounds of NOON donor atoms and their antibacterial and antifungal activity. Arab J Chem 2010;3:103-13.
44. Chohan ZH, Arif M, Akhtar MA, Supuran CT. Metal-based antibacterial and antifungal agents: synthesis, characterization, and *in vitro* biological evaluation of Co(II), Cu(II), Ni(II), and Zn(II) complexes with amino acid-derived compounds. Bioinorg Chem Appl 2006;2006:1-13.
45. Nagesh GY, Mruthyunjayaswamy BHM. Synthesis, characterization and biological relevance of some metal (II) complexes with oxygen, nitrogen, and oxygen (ONO) donor Schiff base ligand derived from thiazole and 2-hydroxy-1-naphthaldehyde. J Mol Struct 2015;1085:198-206.
46. El-Wahab ZHA, Mashaly MM, Salman AA, El-Shetary BA, Faheim AA. Co(II), Ce(III) and UO2(VI) bis-salicylate thiosemicarbazide complexes: binary and ternary complexes, thermal studies and antimicrobial activity. Spectrochim Acta A 2004;60:2861-73.
47. Meyer BN, Ferrigni NR, Putnam JE, Jacobsen LB, Nichols DE, McLaughlin JL. Brine shrimp: a convenient general bioassay for active plant constituents. Planta Med 1982;45:31-4.
48. Petering DH, Sigel H. Carcinostatic copper complexes, in "Metal Ions in Biological Systems" Marcel Dekker (NY); 1980.